PHYSICAL REVIEW D VOLUME 15, NUMBER 7 1 APRIL 1977

Inclusive distributions for sequential decay processes*

L. Durand†
Theoretical Division, Los Alamos Scientific Laboratory, University of California, Los Alamos, New Mexico 87545

P. Fishbane
Physics Department, University of Virginia, Charlottesville, Virginia 22901‡
and Theoretical Division, Los Alamos Scientific Laboratory, University of California, Los Alamos, New Mexico 87545

L. M. Simmons, Jr. and R. Slansky
Theoretical Division, Los Alamos Scientific Laboratory, University of California, Los Alamos, New Mexico 87545
(Received 12 October, 1976)

The multiplicity and inclusive distributions for the sequential decay of a massive state into massless particles are studied, with particular emphasis on polynomial matrix elements. Integral equations for these distributions are derived and discussed, and a Monte Carlo event generator is also described. In many of the models for which the average multiplicity grows linearly with mass, the inclusive spectra are similar to those obtained with a constant matrix element. However, there is also a large class of models in which the momentum spectrum flattens out after falling several decades. The large fluxes, the increase of associated multiplicities, and the large violations of scaling observed in large-transverse-momentum reactions would all receive natural explanations in cluster models with this kind of decay matrix element. The same mechanism gives a satisfactory phenomenology of the small-transverse-momentum events.

I. RATIONALE

Many phenomenological models of multiparticle production suppose that, at an intermediate stage, the final state consists of a few massive objects which subsequently decay into the observed hadrons.[1] In hadronic collisions the objects are often viewed as clusters of particles which are produced peripherally or multiperipherally, and then decay according to some matrix element, usually a constant. In e^+e^- annihilation, the final-state hadrons have been interpreted to be the decay products of a single cluster at lower energies, and to be two jets formed by neutralizing the quark quantum numbers at higher energies.[2]

Many of the models based on these notions are quite useful for interpreting the gross features of multiparticle production. Also, there is positive evidence in hadronic data for the existence of clusters, although estimates of their average multiplicity cover a broad range.[3] This raises a question concerning the universality of the cluster picture and, without sufficiently detailed theoretical guidelines, the answer must rely on phenomenological analyses. Thus there have been many efforts to extend these models to rare but interesting reactions, such as those involving a particle at large transverse momentum k_T.[4]

The purpose of this paper is to analyze the decay characteristics of objects which could appear as clusters. We will assume that the cluster decays by a sequential process into zero-mass particles. As discussed in Sec. II, the ultrarelativistic limit greatly simplifies the kinematics, and the sequential-decay picture permits the derivation of useful equations for the multiplicity distribution and inclusive cross sections. These results could be applied to cluster models, although we will not approach the difficult question of cluster production here.

Many matrix elements lead to inclusive distributions which are similar to those obtained from "flat phase space" (a constant matrix element for each multiplicity). Here the invariant cross section falls a little faster than exponentially with increasing momentum. However, we have also found large classes of models in which the momentum distribution can suddenly flatten (after falling many decades) before taking the final plummet to zero at the edge of phase space. In models where the average multiplicity grows linearly with the mass of the cluster, the low-momentum inclusive spectrum scales approximately. The flattening begins at a fixed momentum independent of the cluster mass. Consequently, sizable violations of scaling will occur at these larger values of momentum.

We expect this kind of cluster decay to give a satisfactory account of large-k_T phenomenology in a model in which the clusters are produced with small transverse momentum. The flattening of the momentum spectrum gives the relatively large flux of particles at large k_T. (If the momentum spectrum drops off exponentially or faster in the cluster rest frame, the relatively large yields at high k_T can be achieved only if the clusters themselves are produced with large k_T.) Moreover, two fea-

tures of the large-k_T data, namely, the large violations of scaling[4] and the increase of associated multiplicity with the k_T of the particle which is observed, are explained naturally if the average cluster mass increases slowly with the total center-of-mass energy. In addition, the faster-than-linear A dependence of the large-k_T yields from nuclear targets can be understood as a multiple-scattering effect within the nucleus, where the cluster mass can be increased by the multiple collisions. At the same time, low-k_T phenomenology is controlled in this picture by the more copiously produced low-mass clusters, and the standard results are easily reproduced. A more unified treatment of both large- and small-k_T processes is an attractive feature of this approach. Work along these lines is currently in progress.

It is also interesting to apply these ideas to hadron production in e^+e^- annihilations. As the e^+e^- energy is increased, the probability of producing a large-momentum particle in the flattened region of the inclusive distribution is also increased. These events will appear jetlike, with the jet axis along the direction of the high-momentum particle. In fact, it is possible to fit the observed sphericities and multiplicities[2] in terms of these single-cluster models.[5] If one assumes that the clusters seen in e^+e^- annihilations are similar to those produced in hadronic collisions, it is then possible to study production of massive lepton pairs. Work is also in progress on this problem.

This paper is organized as follows: Section II contains a compendium of general formulas for the multiplicity and momentum spectra.[6] Our assumptions are discussed and equations for the multiplicity distributions and inclusive cross sections are derived.[7]

The complete solution for flat phase space (constant matrix element) is reviewed in Sec. III, where exact formulas for the multiplicities and one- and two-particle inclusive spectra are derived. We should emphasize that these simple analytic results do not require computer calculations.

Section IV begins the analysis of general sequential decay models. The growth of the average multiplicity with cluster mass is studied, and the conditions which restrict this growth to be no faster than linear with mass are derived. Technically this involves solving the equation for the "weighted volume" of phase space. An outline of the solution is given in Sec. IV, and a number of useful details are included in an Appendix.

The inclusive momentum distribution is discussed in Sec. V, where we present an efficient Monte Carlo method for solving the equations.[8] This approach to dealing with the cluster decay is very powerful and can greatly simplify some model calculations.

A number of examples are shown in Sec. VI, where we also discuss some qualitative aspects of models which give an enhanced large-momentum flux.

II. NOTATION AND ASSUMPTIONS

We set our notation by reviewing some well-known formulas. The probability for a state with four-vector momentum P, $P^2=M^2$, to decay into n particles is proportional to the Lorentz-invariant, weighted volume of n-body phase space,

$$\Gamma_n(P^2)=\int\left(\prod_{i=1}^{n}\frac{d^3k_i}{2E_i}\right)\delta^4\left(P-\sum_{i=1}^{n}k_i\right)\times|M_n(k_1,\ldots,k_n)|^2, \tag{2.1}$$

where $M_n(k_1,\ldots,k_n)$ is the n-particle decay matrix element. The set of functions $\Gamma_n(P^2)$ contains all the available information about the multiplicity distribution as a function of P^2. For many purposes it is convenient to combine the Γ_n into a generating function,[6]

$$\Gamma(\lambda,P^2)=\sum_{n=2}^{\infty}\lambda^{n-2}\Gamma_n(P^2). \tag{2.2}$$

(The choice of the powers of λ simplifies some equations below.) The average decay multiplicity (minus one) at the mass M, $\langle n-1\rangle_M$, is given in terms of $\Gamma(\lambda,M^2)$ by

$$N(M)\equiv\langle n-1\rangle_M=\frac{\partial}{\partial\lambda}[\lambda\,\Gamma(\lambda,M^2)]\Big/\Gamma(\lambda,M^2)\Big|_{\lambda=1}, \tag{2.3a}$$

and the second moment is

$$\langle(n-1)(n-2)\rangle_M=\frac{\partial^2}{\partial\lambda^2}[\lambda\,\Gamma(\lambda,M^2)]\Big/\Gamma(\lambda,M^2)\Big|_{\lambda=1}. \tag{2.3b}$$

The Lorentz-invariant single-particle momentum distribution for the n-body decay is proportional to

$$2E\frac{d\Gamma_n}{d^3k}=\sum_{j=1}^{n-2}2E\frac{d\Gamma_n^{(j)}}{d^3k}, \tag{2.4a}$$

where

$$2E\frac{d\Gamma_n^{(j)}}{d^3k}=\int\left(\prod_{i=1}^{n}\frac{d^3k_i}{2E_i}\right)\delta^4\left(P-\sum_{i=1}^{n}k_i\right)\times 2E_j\delta^3(\vec{k}-\vec{k}_j)\,|M_n(k_1,\ldots,k_n)|^2. \tag{2.4b}$$

For future convenience we have not included particles n and $n-1$ in the sum. The Lorentz-invari-

ant inclusive cross section is

$$f(P^2,(P-k)^2)=2E\frac{dN}{d^3k}=\sum_{n=3}^{\infty}2E\frac{d\Gamma_n}{d^3k}\Big/\Gamma(M^2),$$
$$\Gamma(M^2)=\Gamma(\lambda=1,M^2), \tag{2.5}$$

normalized such that

$$\int\frac{d^3k}{2E}f(P^2,(P-k)^2)=\langle n-2\rangle_M. \tag{2.6}$$

More complicated correlation functions are easily written down in a similar fashion.

For a general decay matrix element $M_n(k_1,\ldots,k_n)$, the multiplicity and inclusive distributions must be computed directly from Eqs. (2.1) and (2.5). In this paper, we study these distributions in a restricted set of models. We assume the following:

(1) The n decay products are all massless. The ultrarelativistic limit greatly simplifies the multiple integrals of Eqs. (2.1) and (2.4). For example, if $|M_n|^2$ is a constant, the integrals are elementary functions. This is not so for the massive case.[6] This assumption is quite reasonable for decays into energetic pions, but will fail for particle production near the edge of phase space and for decays into very massive particles.

(2) The clusters decay sequentially as indicated in Fig. 1. This assumption means that $|M_n(k_1,\ldots,k_n)|^2$ can be broken up into a product of $n-1$ terms, where each term corresponds to a vertex in the sequential decay.

(3) The probability distribution associated with each vertex depends only on the masses of the adjoining particles (and not on the preceding momenta), so that

$$|M_n(k_1,\ldots,k_n)|^2=\prod_{i=1}^{n-1}|F(M_{i-1}^2,M_i^2)|^2, \tag{2.7}$$

where $M_0=M$ and $M_{n-1}=0$. (Note that this matrix element is already totally symmetric in the momenta so no explicit Bose symmetrization is necessary.) There are some models for which it is trivial to relax this assumption; and it is particularly simple to do so using the Monte Carlo method of calculation discussed in Sec. V.

Probabilities of this form do not necessarily exclude cases in which the intermediate particles in the decay sequence have spin, since polarization sums can eliminate angular dependence. For example, suppose $M_0,M_1,M_2,\ldots,M_{n-1}$ are all spin $\frac{1}{2}$ and M_0 and M_{n-1} are unpolarized. Then matrix elements of the forms $g\bar{u}u$, $g\bar{u}\gamma_5 u$, or $g\bar{u}\gamma_5\not{k}u$ at each vertex lead to Eq. (2.7) with

$$|F(M^2,M_1^2)|^2=g^2(M+M_1)^2/MM_1,$$
$$|F(M^2,M_1^2)|^2=g^2(M-M_1)^2/MM_1,$$

and

$$|F(M^2,M_1^2)|^2=g^2(M^2-M_1^2)^2/2MM_1,$$

respectively. The model with spin-1 sequential decay is easily analyzed with our formalism, but does not satisfy assumption (3).[5]

The sequential-decay picture, Eq. (2.7), allows Eq. (2.1) to be written as a (well-known) recurrence relation,[6]

$$\Gamma_n(M^2)=\frac{\pi}{2M^2}\int_0^{M^2}dM_1^2(M^2-M_1^2)|F(M^2,M_1^2)|^2\times\Gamma_{n-1}(M_1^2), \tag{2.8a}$$

with

$$\Gamma_2(M^2)=\frac{\pi}{2}|F(M^2,0)|^2. \tag{2.8b}$$

Equation (2.8) can be converted into an integral equation for $\Gamma(\lambda,M^2)$ by multiplying $\Gamma_n(M^2)$ by λ^{n-2} and summing from $n=3$ to ∞,

$$\Gamma(\lambda,M^2)=\Gamma_2(M^2)+\frac{\pi\lambda}{2M^2}\int_0^{M^2}dM_1^2(M^2-M_1^2)|F(M^2,M_1^2)|^2\times\Gamma(\lambda,M_1^2). \tag{2.9}$$

The Lorentz invariance of $\Gamma(\lambda,M^2)$ is manifest, and the series solution of Eq. (2.9) converges so long as Eqs. (2.1) and (2.2) make sense. Equation (2.9) has two important applications in our work. The asymptotic form of the multiplicity distribution for large M^2 can be found directly from Eq. (2.9). Moreover, the solution of Eq. (2.9) is necessary for the inclusive-cross-section calculations carried out in Secs. V and VI.

It is convenient to rewrite Eq. (2.9) in dimensionless form, since $|F(M^2,M_1^2)|^2$ has units of in-

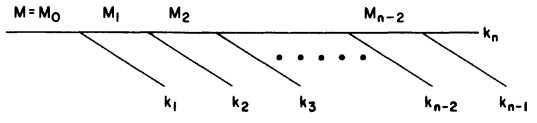

FIG. 1. Sequential decay process. This figure shows the labeling conventions used in this paper. Each vertex corresponds to a factor $|F(M^2,M_1^2)|^2$. The external particles with momenta $k_1,\ldots,k_n$ are all massless.

verse mass squared. Let

$$|F(M^2,M_1^2)|^2=\frac{g^2}{2\pi}p(y,z),$$
$$y=Mg/2,\quad z=M_1/M, \tag{2.10}$$
$$\Gamma(\lambda,M^2)=\tfrac{1}{4}g^2\gamma_\lambda(y),$$

where g is a coupling constant with units of inverse mass. Equation (2.9) becomes

$$\gamma_\lambda(y)=p(y,0)+2\lambda y^2\int_0^1 dz\,z(1-z^2)p(y,z)\gamma_\lambda(yz). \tag{2.11}$$

This equation is further discussed in Secs. IV and V and the Appendix.

It is also quite straightforward to derive an equation for the inclusive cross section,[7] as defined in Eqs. (2.4) and (2.5). (The modifications needed to include the last two particles on the chain in Fig. 1 are trivial, but make the equation less neat in appearance.) We will not make much use of the integral equation for the inclusive cross section in this paper, and some readers may wish to go directly to Sec. III.

The invariant cross section, $f(P^2,(P-k)^2)$, can be written as

$$G(P^2,(P-k)^2)\equiv\Gamma(P^2)f(P^2,(P-k)^2)=2E\sum_{n=3}^{\infty}\sum_{j=1}^{n-2}\frac{d\Gamma_n^{(j)}}{d^3k}. \tag{2.12}$$

The function $d\Gamma_n^{(j)}/d^3k$ defined in Eq. (2.4b) can be identified for the sequential decay as the momentum distribution of the jth particle off the chain in the n-body decay in Fig. 1. It is convenient to reorganize this sum and consider the distribution of the jth particle off the chain, summed over all multiplicities,

$$G^{(j)}(P^2,(P-k)^2)=2E\sum_{n=j+2}^{\infty}\frac{d\Gamma_n^{(j)}}{d^3k}, \tag{2.13}$$

so that

$$G(P^2,(P-k)^2)=\sum_{j=1}^{\infty}G^{(j)}(P^2,(P-k)^2). \tag{2.14}$$

A substitution of Eq. (2.7) into Eqs. (2.4b) and (2.13) yields

$$G^{(1)}(P^2,(P-k)^2)=\int dM_1^2\,|F(M^2,M_1^2)|^2\delta_+\times(M_1^2-(P-k)^2)\,\Gamma(M_1^2). \tag{2.15}$$

[The two-body decay can be included by replacing $\Gamma(M_1^2)$ by $\bar{\Gamma}(M_1^2)=2\delta(M_1^2)+\Gamma(M_1^2)$.] The $G^{(j)}(P^2,(P-k)^2)$, for $j>1$, are somewhat more complicated, but can be written as

$$G^{(j)}(P^2,(P-k)^2)=\int dm^2\,2E\frac{d\Gamma_{j+1}^{(j)}(P^2,m^2)}{d^3k}\Gamma(m^2), \tag{2.16}$$

where $d\Gamma_{j+1}^{(j)}(P^2,m^2)/d^3k$ is the distribution of the jth particle off the chain in a $(j+1)$-body decay of a cluster of mass P^2 and the mass of the $(j+1)$th body is m. This is an auxiliary object, but it is useful because it satisfies the recurrence relation,

$$2E\frac{d\Gamma_{j+1}^{(j)}(P^2,m^2)}{d^3k}=\int d^4q\,|F(P^2,q^2)|^2\delta_+((P-q)^2)\times 2E\frac{d\Gamma_j^{(j-1)}((P-q)^2,m^2)}{d^3k}. \tag{2.17}$$

In effect, Eq. (2.17) shows how to add a zero-mass particle to the front of the chain in Fig. 1, where q is the four-vector momentum of the cluster after this first particle has been emitted. A linear integral equation for $G(P,k)$ is now easily derived by summing Eq. (2.16) from $j-2$ to ∞, using the definition Eq. (2.14), and substituting Eq. (2.17) into the right-hand side of Eq. (2.16). The invariant form of the resulting equation is

$$G(P^2,(P-k)^2)=G^{(1)}(P^2,(P-k)^2)+\int d^4q\,|F(P^2,q^2)|^2\delta_+((P-q)^2)\times G(q^2,(q-k)^2). \tag{2.18}$$

Two of the integrals can be evaluated in the frame $P=(M,\vec{0})$, where rotational invariance is simple:

$$G(M^2,\xi)=|F(M^2,\xi)|^2\Gamma(\xi)+\frac{\pi}{2M^2x}\times\int_0^{\xi'}d\xi'\int_{M_l^2}^{M_u^2}dM_1^2\,|F(M^2,M_1^2)|^2G(M_1^2,\xi'), \tag{2.19}$$

where

$$x=2k/M,\quad 0\le x\le 1,\quad \xi=M^2(1-x),\quad 0\le\xi\le M^2,$$
$$M_u^2=\xi'+xM^2, \tag{2.20}$$
$$M_l^2=\xi'/(1-x).$$

This equation has proved to be useful on occasion, although the solutions presented in Sec. VI were obtained by Monte Carlo techniques.

III. CONSTANT MATRIX ELEMENT

Our object in this section is to give a complete presentation of "flat phase space," subject to the assumptions of Sec. II. Many of the results are

well known, but a careful presentation will ease the more complicated discussions in Secs. IV and V, and we thought it useful to collect these results in one place.

All the formulas of Sec. II are easily evaluated for

$$|F(M^2, M_1^2)|^2 = \frac{g^2}{2\pi}. \tag{3.1}$$

$\Gamma_n(M^2)$ is then the multiple integral,

$$\Gamma_n(M^2) = \left(\frac{g^2}{2\pi}\right)^{n-1} \int \left(\prod_{i=1}^{n} \frac{d^3k_i}{2E_i}\right) \delta^4\left(P - \sum_{i=1}^{n} k_i\right). \tag{3.2}$$

There are many ways to evaluate Eq. (3.2),[6] but perhaps the simplest is to make a change of variables to the intermediate mass variables, $M_1, M_2, \ldots, M_{n-2}$ of Fig. 1, do the angular integrations, and then transform to scaled variables $y_i = M_i/M_{i-1} (M_0 = M)$. The $(n-2)$-fold mass integration then becomes a product of elementary β functions, and $\Gamma_n(M^2)$ is easily reduced to

$$\Gamma_n(M^2) = \frac{1}{M^2} y^{2n-2} \frac{1}{(n-1)!\,(n-2)!}, \tag{3.3}$$

where $y = Mg/2$, as in Eq. (2.10), and $n = 2, 3, \ldots$.

We first study the multiplicity distribution. $\Gamma_n(M^2)$ is proportional to the probability of an n-body decay. The normalization sum is

$$\Gamma(M^2) = \sum_n \Gamma_n(M^2) = (y/M^2) I_1(2y), \tag{3.4a}$$

where I_k is the modified Bessel function,

$$I_k(z) = \sum_{l=0}^{\infty} \frac{(z^2/4)^{l+k/2}}{l!\,(l+k)!}. \tag{3.4b}$$

The large-z behavior of $I_k(z)$ is given by the asymptotic formula

$$I_k(z) \sim \frac{e^z}{(2\pi z)^{1/2}} \left[1 - \frac{4k^2-1}{8z} + \frac{(4k^2-1)(4k^2-9)}{128z^2} \cdots\right]. \tag{3.5}$$

From Eqs. (3.3) and (3.4), the normalized multiplicity distribution is

$$P_n = \frac{y^{2n-3}}{(n-1)!\,(n-2)!} \frac{1}{I_1(2y)}, \quad n = 2, 3, \ldots \tag{3.6}$$

where P_n is the probability that a cluster of mass M and coupling g [Eq. (3.1)] will decay into n particles. It should be noted that Eq. (3.6) is not a Poisson distribution, even though, because of Eq. (3.1), this is an "independent-emission model." Energy-momentum conservation in Eq. (3.2) induces correlations which do not vanish for large y; that is, Eq. (3.6) does not approach a Poisson distribution as $y \to \infty$. This distribution is always narrower than a Poisson distribution and for some calculations the difference is appreciable: The probability of n being much different from average is greatly suppressed compared to a Poisson distribution. In a model where P_n is a Poisson distribution and $|M_n|^2$ is constant, $|M_n|^2$ therefore cannot be written in the form Eq. (2.7).

From Eqs. (3.3), (2.2), and (2.10), it is easy to calculate the multiplicity generating function $\gamma_\lambda(y)$,

$$\gamma_\lambda(y) = I_1(2\lambda^{1/2}y)/(\lambda^{1/2}y). \tag{3.7}$$

The form Eq. (3.7) satisfies Eq. (2.11). The average multiplicity, $\langle n-1\rangle_M = N(M)$, is given by

$$N(M) = yI_0(2y)/I_1(2y) \simeq y + \frac{1}{4} + \frac{3}{32y} + O\left(\frac{1}{y^2}\right), \quad y \gg 1. \tag{3.8}$$

The approach to a linear mass-multiplicity relationship for flat phase space is extremely rapid: At $y = 3$, the error in $N(M) = y + \frac{1}{4}$ is just 1%.

The second moment of the multiplicity distribution is given exactly by

$$\langle (n-1)(n-2)\rangle_M = y^2. \tag{3.9}$$

Higher moments are again ratios of Bessel functions. The asymptotic behavior for large y of $\langle n^P\rangle_M$ is y^P. Equations (3.8) and (3.9) suffice to show that P_n [Eq. (3.6)] is narrower than a Poisson distribution, since

$$f_2 = \langle (n-1)(n-2)\rangle - \langle (n-1)\rangle^2 \simeq -\tfrac{1}{2}y - \tfrac{1}{4}$$

($f_2 = 0$ for Poisson).

Although the inclusive cross section can be derived by solving Eq. (2.19), it is much simpler to note that, since the decay matrix element is independent of intermediate cluster masses M_i, the first particle off the chain has the same momentum distribution as any other. Thus, from Eq. (2.4), with $\xi = (P-k)^2$,

$$2E\frac{d\Gamma_n}{d^3k} = \frac{g^2}{2\pi}(n-2)\Gamma_{n-1}(\xi). \tag{3.10}$$

The inclusive distribution, normalized to $\langle n-2\rangle$, is obtained by substituting Eq. (3.3) into Eq. (3.10) and summing it from $n = 2$ to ∞:

$$2E\frac{dN}{d^3k} = \frac{g^3 M}{4\pi} \frac{I_0(g\xi^{1/2})}{I_1(Mg)}. \tag{3.11}$$

It is easily checked that $G(M^2, \xi) = g^4 I_0(g\xi^{1/2})/(8\pi)$ satisfies Eq. (2.19).

The asymptotic form of Eq. (3.11) is useful, since the Bessel functions approach their asymptotic limits very rapidly. For k not too near $M/2$,

Eq. (3.11) becomes

$$2E\frac{dN}{d^3k}\simeq\frac{g^2}{2\pi}\frac{y}{(1-x)^{1/4}}\exp\{-2y[1-(1-x)^{1/2}]\},\tag{3.12}$$

for $2y(1-x)^{1/2}\gg 1$, where we remind the reader that $y=Mg/2$ and $x=2k/M$, $0\leq x\leq 1$. For small k, the spectrum falls as $\exp(-gk)$. The decrease is more rapid for larger k. One phenomenological implication of this result for cluster models with constant decay matrix elements is that the observed large-transverse-momentum yields can only be obtained by imparting significant transverse motion to the cluster. However, this is not a general feature of all sequential-decay models.

A convenient characterization of the momentum distribution is in terms of the moments $\langle k^j\rangle$, which are easily calculated from Eq. (3.11):

$$\langle(gk)^j\rangle=(j+1)!\,I_{j+1}(2y)/I_1(2y).\tag{3.13}$$

The dispersion in k is defined by

$$D^2=\frac{\langle k^2\rangle-\langle k\rangle^2}{\langle k\rangle^2}\simeq\frac{1}{2}\left(1-\frac{3}{2y}\right),\quad y\gg 1.\tag{3.14}$$

Another easily calculable quantity in this case is the two-particle distribution function. The two-particle spectrum for the first two particles off the chain is the same as that for any other pair (for a constant matrix element). For an n-body decay (but ignoring the last two particles), there are $\frac{1}{2}(n-2)(n-3)$ pairs. The calculation is similar to that leading to Eq. (3.11),

$$2E_1 2E_2\frac{d^6N}{d^3k_1 d^3k_2}=\frac{Mg^6}{16\pi^2}\frac{[(P-k_1-k_2)^2]^{1/2}}{I_1(2y)}\times I_1\{g[(P-k_1-k_2)^2]^{1/2}\}.\tag{3.15}$$

The n-body distribution functions are computed in a similar fashion. We should note that all these distributions are easily used in model calculations because of their manifest Lorentz-transformation properties.

The associated multiplicity is also easily calculable. There are two common definitions of this quantity. The first definition we consider is that the associated multiplicity $A(k)$ is the average number of additional particles produced, given that one particle is observed to have momentum k:

$$A(k)=y(1-x)^{1/2}\frac{I_0(2y(1-x)^{1/2})}{I_1(2y(1-x)^{1/2})}\underset{y\to\infty}{\sim}y(1-x)^{1/2}.\tag{3.16}$$

This quantity decreases with increasing k.

A second definition is that $[\tilde{A}(k)]^2$ is the average number of pairs where one secondary has momentum k, divided by the average number of particles at k:

$$\tilde{A}(k)=y(1-x)^{1/2}.\tag{3.17}$$

Regardless of the definition of the associated multiplicity, it is still necessary to fold it with the mass spectrum to see whether it should grow or decrease with the momentum of the observed particle.

Finally, we wish to point out that there exists a class of models which appear to be nontrivial but are in fact not essentially different from flat phase space. Any matrix element $|F(M^2,M_1^2)|^2$ of the form

$$|F(M^2,M_1^2)|^2=\alpha(M^2)/\alpha(M_1^2)\tag{3.18}$$

gives, by virtue of our sequential-decay assumption,

$$|M_n(k_1,\ldots,k_n)|^2\propto\alpha(M^2)/\alpha(0).\tag{3.19}$$

Although the resulting $\Gamma(M^2)$ has a more complicated M dependence, the inclusive and multiplicity distributions are identical to flat phase space. The common factor $\alpha(M^2)$ can be absorbed into the (unknown) cluster-production probability.

IV. NONCONSTANT DECAY MATRIX ELEMENTS

The problem of obtaining multiplicity distributions and inclusive cross sections for nonconstant $|F(M^2,M_1^2)|^2$ is more difficult. In this section we focus on the multiplicity distribution by studying the solution of Eq. (2.11). The following two sections are then devoted to the inclusive cross sections.

In outline, our approach to solving Eq. (2.11) is to assume a power series for $\gamma_\lambda(y)$, and derive a recurrence relation for the coefficients. [We will restrict the choice of $|F(M^2,M_1^2)|^2$ so that this is feasible.] The asymptotic behavior of the average multiplicity can be derived directly from the recurrence relation by methods which are discussed in detail in the Appendix. The recurrence relation also provides a convenient way to evaluate $\gamma(y)$ and $N(M)$ for all y. This solution for $\gamma(y)$ is used to compute the inclusive cross section in the next section.

We restrict our attention to those $|F(M^2,M_1^2)|^2$ which can be approximated by a polynomial in M and M_1,

$$|F(M^2,M_1^2)|^2=\frac{g^2}{2\pi}\sum_{m,n}c_{mn}\left(\frac{g}{2}\right)^{m+n}M^m M_1^n,$$

or [cf. Eq. (2.10)]

$$p(y,z)=\sum_{m,n}c_{mn}\,y^{m+n}z^n.\tag{4.1}$$

The sums on m and n are finite, and may include negative values of m and n so long as the integral in Eq. (2.11) is finite. The c_{mn} must be such that $p(y,z)$ is non-negative. The restriction to polynomial matrix elements is a useful one because $\gamma_\lambda(y)$ is determined by a finite range of M_1 ($M_1 < M$), and $|F(M^2, M_1^2)|^2$ can be fitted arbitrarily accurately by a polynomial of the form Eq. (4.1).

Assume that $\gamma_\lambda(y)$ can be expressed as a power series,

$$\gamma_\lambda(y) = \sum_{n=-1}^{\infty} g_n \frac{y^n}{(n+1)!}, \tag{4.2}$$

where g_n are constants which depend on λ, and the lower limit on the sum is determined by the requirement that the integral in Eq. (2.11) converges. (In many models g_{-1} is zero.) When Eqs. (4.1) and (4.2) are substituted into Eq. (2.11), we find a recurrence relation for the g_n of the form

$$g_n = \lambda \sum_{i=1}^{I} g_{n-i} A_i(n), \tag{4.3}$$

plus inhomogeneous terms for $n \leq I$.

It is possible to find the asymptotic behavior of the average multiplicity $N(M)$ from the asymptotic form of the recurrence relation for g_n and the results in the Appendix. The basic results we need here are the following: The series is convergent if $|A_i(n)| < cn^i$ for $n \to \infty$. However, if any of the $A_i(n)$ grows with n as $n \to \infty$, $N(M)$ will grow faster than linearly in mass. If the largest $A_i(n)$ approaches a positive constant as n increases, $N(M)$ grows linearly. Finally, if all the $A_i(n)$ go to zero for $n \to \infty$, $N(M)$ will grow less rapidly than linearly.

Models where $N(M)$ grows faster than linearly for large M are unphysical for real, finite-mass particles. This possibility is an artifact of the ultrarelativistic approximation. It is, therefore, useful to impose on the c_{mn} in Eq. (4.1) the constraints which require each $A_i(n)$ to approach a constant for large n. These constraint equations can be given a general solution in terms of the following combination of variables:

$$(M + M_1)/M = 1 + z$$

and

$$\tfrac{1}{2} g(M - M_1) = y(1 - z). \tag{4.4}$$

The most general expansion of $p(y,z)$ of the form Eq. (4.1) for which the average multiplicity grows no faster than linearly in y is

$$p(y,z) = \sum_{k,l} p_{k,l} (1+z)^k (1-z)^l y^l, \tag{4.5}$$

where again the sum on k and l is finite, some negative values of k and l are allowed, and $p(y,z)$ must be non-negative.

Upon substituting Eqs. (4.2) and (4.5) into Eq. (2.11), evaluating some elementary integrals, and readjusting the summation indices, we derive the recurrence relation for the g_n,

$$g_n = (n+1)! \sum_j p_{n,j} + \lambda \sum_{i=1}^{I} g_{n-i} A_i(n). \tag{4.6}$$

Since the sums in Eq. (4.5) are finite, the inhomogeneous term is absent from Eq. (4.6) for large n. By explicit calculation, $A_i(n)$ is given by

$$A_i(n) = 2 \sum_k p_{k,i-2} \frac{(n+1)!}{(n-i+1)!} \int_0^1 dz\, z^{n-i+1} (1+z)^{k+1} (1-z)^{i-1}$$

$$= 2 \sum_k \sum_{j=0}^{k+1} p_{k,i-2} \left[\frac{(n+1)!\,(n-i+j+1)!}{(n-i+1)!\,(n+j+1)!}\right] \left[\frac{(k+1)!\,(i-1)!}{j!\,(k+1-j)!}\right]. \tag{4.7}$$

The large-n limit of this expression is

$$A_i(n) \xrightarrow[n \to \infty]{} A_{i,0} = 4(i-1)! \sum_k 2^k p_{k,i-2}, \tag{4.8}$$

which is a constant, as it should be.

Models for which $N(M)$ is asymptotically a linear function of y have at least one $A_{i,0} \neq 0$. The asymptotic recurrence relation is

$$g_n \sim \lambda \sum_{i=1}^{I} g_{n-i} A_{i,0}. \tag{4.9}$$

As discussed in the Appendix, $\gamma_\lambda(y)$ grows exponentially in this case,

$$\gamma_\lambda(y) \sim [\mu(\lambda) y]^{\alpha(\lambda)} e^{\mu(\lambda) y}. \tag{4.10}$$

As is shown in the Appendix, $\mu(\lambda)$ is obtained from the asymptotic solution to Eq. (4.6), and is the root of the polynomial equation,

$$[\mu(\lambda)]^I = \lambda \sum_{i=1}^{I} A_{i,0} [\mu(\lambda)]^{I-i}, \tag{4.11}$$

with the largest positive real part. From Eqs. (2.3) and (4.10), we find that

$$N(M) \sim \mu' y + \alpha \mu'/\mu + \alpha' \ln \mu y, \tag{4.12}$$

where primes denote derivatives with respect to λ, and all quantities are evaluated for $\lambda = 1$.

For some explicit examples of the above solutions we make an inessential simplification, and assume that $|F(M^2, M_1^2)|^2$ is a power series in the momentum $(M^2 - M_1^2)/(2M)$ of the emitted particle in the rest frame of M. In other words, in Eq. (4.5) we let

$$p_{k,I} = \delta_{k,I} p_{k,I} \equiv \delta_{k,I} p_k, \tag{4.13}$$

where p_k can be nonzero for $k = -1, 0, \ldots, I-2$, and must satisfy the positivity constraints. Equation (4.6) then becomes

$$g_n = (n+1)!\, p_n + \lambda \sum_{i=1}^{n+1} g_{n-i}\, A_i(n) \tag{4.14a}$$

for $-1 \leq n \leq I-2$, and

$$g_n = \lambda \sum_{i=1}^{I} g_{n-i}\, A_i(n) \tag{4.14b}$$

for $n > I-2$, where

$$A_i(n) = (i-1)!\, 2^i p_{i-2} \prod_{k=1}^{i} \left(\frac{n-i+1+k}{n-i+2k} \right). \tag{4.15}$$

Equations (4.14), (4.15), and (4.2) completely specify $\gamma_\lambda(y)$. As an example, suppose

$$|F(M^2, M_1^2)|^2 = \frac{g^2}{2\pi} \left(g\, \frac{M^2 - M_1^2}{2M} \right)^N = \frac{g^2}{2\pi} y^N (1-z^2)^N. \tag{4.16}$$

Then Eq. (4.12) becomes

$$[\mu(\lambda)]^{N+2} = 2^{N+2}(N+1)!\,\lambda \tag{4.17a}$$

or

$$\mu(\lambda) = 2(\lambda)^{1/(N+2)} [(N+1)!]^{1/(N+2)}. \tag{4.17b}$$

The average multiplicity then goes asymptotically as

$$N(M) = \frac{2y}{N+2} [(N+1)!]^{1/(N+2)} + \text{constant}. \tag{4.18}$$

More complicated cases require solving Eq. (4.12) for $\mu(\lambda)$. In the cases where $|F|^2 \sim k^N$, Eq. (4.16), the asymptotic behavior for $N(M)$ is reached for rather low y. However, if $|F|^2$ has local minima in k, the asymptotic formula is not a good approximation until M is above the region where $|F|^2$ shows this structure.

V. CALCULATING THE INCLUSIVE SPECTRUM

It is very difficult to solve Eq. (2.19) directly for the inclusive cross section, or even to obtain asymptotic information from it. We therefore turn to numerical methods, since our primary purpose is to examine the dependence of the shape of $2E dN/d^3k$ on variations of $|F|^2$. The method presented here is a Monte Carlo technique[8] in which entire events are generated with the quantum-mechanical probability Eq. (2.7) constrained by phase space. These events may then be analyzed as if they were experimental data. This method is particularly convenient if one must include experimental cuts, resolutions, and so forth in order to compare model calculations with data. It is also a simple matter to compute complicated correlation functions. However, it is somewhat awkward to study the functional dependence of these correlations on the parameters of the model and make best fits to the data. The sequential-decay hypothesis makes it possible to alleviate this problem somewhat, since a very fast and simple event generator can be constructed.

The input for the event generator includes the cluster mass M, a table of $P_2(M')$, the probability that a cluster of mass $M' \leq M$ will decay into two zero-mass particles, and $P(M_1|M')$, the probability distribution for a cluster of mass M' to decay into a zero-mass particle and a cluster of mass M_1 $(0 < M_1 < M' \leq M)$. These tables are easily constructed in terms of $\Gamma(M^2)$, as we will show in this section. The output generated for each event includes the multiplicity (this is not determined *a priori*), and a list of four-vectors, one for each final-state particle, which satisfy energy-momentum conservation.

The order of our presentation is first to describe the procedure followed in generating an event, assuming that $P_2(M')$ and $P(M_1|M')$ are known, and then to describe the evaluation of $P_2(M')$ and $P(M_1|M')$. The next section discusses some results of explicit calculations.

We first generate a series of masses $M_1, M_2, \ldots, M_{n-2}$, as labeled in Fig. 1. We start with mass M. The probability of a cluster of mass M undergoing a two-body decay into zero-mass particles is $P_2(M)$. We generate a uniform random number r on the interval (0, 1). If $r < P_2(M)$ the decay series ends and $M_1 = 0$. If $r > P_2(M)$, M does not decay into two zero-mass particles, and the residual mass after the first decay is nonzero, $M_1 > 0$. An easy and efficient way to generate this residual mass is as follows. We normalize the known function $P(M_1|M)$ so that its maximum value is 1, generate a trial mass M_1 according to a uniform distribution on $(0, M)$, and compute $P(M_1|M)$. We then generate a random number r' on (0, 1). If $r' < P(M_1|M)$, we use the trial value of M_1; otherwise we repeat the procedure. Once M_1 is generated, we ask if M_1 decays into two zero-mass particles. If not, we generate M_2 from $P(M_2|M_1)$. The sequence ends when M_{n-2} decays

into two zero-mass particles. It should be emphasized that the multiplicity distribution is already folded into $P(M_1|M)$ and is not directly needed for the calculation.

The second part of the event generation consists of obtaining a set of n four-vectors from the $n-2$ masses. We start in the M rest frame. The magnitude of the momentum is $k_1=(M^2-M_1^2)/(2M)$. Since the decay has been assumed to be isotropic, we may randomly choose a direction for $\vec{k}_1$. (It is also possible to include a nontrivial angular distribution in the decay.) The recoil cluster (M_1) has momentum $-\vec{k}_1$. We also generate the Lorentz transformation L_1 which transforms vectors from the M_1 rest frame into vectors in the M rest frame. In the M_1 rest frame k_2 has magnitude $(M_1^2-M_2^2)/(2M_1)$ and its direction is again uniform over the unit sphere. This vector is then transformed to the M rest frame by computing L_1k_2. We define L_2 as the Lorentz transformation from the M_2 rest frame to the M_1 rest frame. Then the transformation from the M_2 rest frame to the M rest frame is L_1L_2, and this will be used to transform k_3 to the M rest frame. We continue this procedure down to M_{n-2}. The last step involves generating k_{n-1} and k_n ($\vec{k}_n=-\vec{k}_{n-1}$ in the M_{n-2} rest frame) and transforming both of these back to the M rest frame with $L_1L_2\cdots L_{n-3}L_{n-2}$. This set of n four-vectors satisfies the constraints of energy-momentum conservation. The computing time for N events is proportional to $\langle n-1\rangle$. The CDC 7600 generates a little over 4000 four-vectors per second.

The probability $P_2(M)$ is given simply by

$$P_2(M)=\Gamma_2(M)/\Gamma(M)=p(y,0)/\gamma_1(y), \tag{5.1}$$

where $\Gamma_2(M)$ is given in Eq. (2.8) and $\Gamma(M)$ is the solution to Eq. (2.9) for $\lambda=1$, and $p(y,z)$ and $\gamma_\lambda(y)$ are defined in Eq. (2.10).

The distribution $P(M_1|M)$ is obtained by averaging $P_n(M_1|M)$ over all n, where $P_n(M_1|M)$ is the probability density that a cluster of mass M and preassigned multiplicity n will decay into a zero-mass particle and a cluster of mass M_1. It satisfies the relation

$$\int_0^M dM_1\,P_n(M_1|M)=1. \tag{5.2}$$

Upon comparing Eq. (5.2) with Eq. (2.8), we find that

$$P_n(M_1|M)=\frac{\pi M_1}{M^2}(M^2-M_1^2)\,|F(M^2,M_1^2)|^2 \times\frac{\Gamma_{n-1}(M_1^2)}{\Gamma_n(M^2)}. \tag{5.3}$$

This identification is justified by the definition of $\Gamma_n(P^2)$ in terms of $|M_n|^2$ in Eq. (2.1). To average $P_n(M_1|M)$ over all $n\geq 3$, we multiply Eq. (5.3) by $\Gamma_n(M^2)/[\Gamma(M^2)-\Gamma_2(M^2)]$, which is the probability that a cluster of mass M will actually decay into n particles, and then sum from $n-3$ to ∞. The cancellation of the $\Gamma_n(M^2)$ and the simple form of Eq. (5.3) are explicitly due to the sequential decay hypothesis. Thus, we arrive at the result

$$P(M_1|M)=\frac{\pi M_1}{M^2}(M^2-M_1^2)\,|F(M^2,M_1^2)|^2 \times\frac{\Gamma(M_1^2)}{\Gamma(M^2)-\Gamma_2(M^2)}, \tag{5.4}$$

and the calculation of $P(M_1|M)$ is reduced to computing $\Gamma(M^2)$. It follows from Eq. (2.9) with $\lambda=1$ that $P(M_1|M)$ is normalized to 1. If the method described above is used for generating M_1, all that is needed is

$$P(M_1|M)\propto y_1(y,y_1^2)p(y,y_1)\gamma_1(y_1), \tag{5.5}$$

where $y_1=M_1g/2$, and the other notation is defined in Eq. (2.10). The function $\gamma_1(y)$ is easily calculated from Eq. (4.2) using the coefficients g_n determined by the recurrence relation Eq. (4.3).

VI. SOME EXPLICIT RESULTS

One of the main points of this paper is to show that there exist sequential-decay models whose inclusive distributions differ appreciably from those resulting from the model with a constant matrix element (Sec. III). Both the k_T and M dependences are interesting. For example, if the large-k_T particles observed in hadron scattering originate from clusters with small transverse momentum, dN/dk_T^2 must be much larger at large k_T than computed in the "constant" model. Moreover, the violations of scaling at large k_T in the hadronic data are very large, and this must be reflected in corresponding variations in dN/dk_T^2 as a function of M at fixed k_T. In order to illustrate these effects, we will compare the constant model with several other models. (A more quantitative analysis of the data is in progress.) We will also give a qualitative explanation of why our model matrix elements produce these distributions.

The calculations reported in Figs. 2–5 were performed using the Monte Carlo method of Sec. V. Among the checks made on that procedure, we generated for several M values 50 000 events with constant $|F|^2$ and compared the momentum distribution with the exact formula, Eq. (3.11). The variations were consistent with statistics.

The figures show the single-particle transverse-momentum distributions for different $|F|^2$. After each event is generated, the magnitude of the momentum transverse to the z axis is computed for each final-state particle, and is histogrammed into

bins of 0.1-GeV width. (Perhaps we should recall that, owing to the energy-momentum-conservation constraints, there is no simple relation between the k and k_T distributions.) Each curve incorporates 50 000 multiparticle events and thus includes 50 000 times $\langle n-1\rangle$ values of k_T. Thus, in the domain where $dN/dk_T^2 \sim 0.01$ GeV^{-2}, the statistical error in each bin is $\sim 5\%$.

Figure 2 shows dN/dk_T^2 for $|F|^2 = g^2/2\pi$, $g = 3.3$ GeV^{-1}, plotted in the cluster rest frame. The lower curve is for $M = 5$ GeV, where $\langle n-1\rangle_{5\ \mathrm{GeV}} = 8.5$, and the upper curve is for $M = 9$ GeV, where $\langle n-1\rangle_{9\ \mathrm{GeV}} = 15.1$. The downward curvature indicates that the distribution falls faster than $\exp(-ak_T)$, although $\exp(-4k_T)$ fits dN/dk_T^2 fairly well for $k_T \lesssim 1.5$ GeV. For low k_T these curves exhibit approximate scaling in M, but the scaling violation increases with increasing k_T. (This is clearly an edge-of-phase-space effect.) In models based on clusters of this type, the naive extrapolation, $2E dN/d^3k \sim \exp(-ak_T)$, obtained from fitting the low-k_T data, is in fact an upper limit on the large-k_T flux. Thus the value of dN/dk_T^2 at large k_T is much too small to account for the large-k_T production seen in the hadronic data, unless the clusters themselves are given a large k_T. Of course, it could be that high transverse momentum of the clusters is the physical origin of the large yields of large-k_T particles. But it is one purpose of this paper to suggest an alternative phenomenology in which the clusters are themselves produced with low k_T, but their decay mechanisms yield adequate numbers of large-k_T secondaries. An advantage of this viewpoint is the possible unification with the hadronic clusters formed in e^+e^- annihilations.[5]

At large k_T, the model in Fig. 3 shows large violations of scaling, and a large flux (compared to Fig. 2) for the more massive cluster. The matrix element in this case is

$$|F(M^2, M_1^2)|^2 = \frac{g^2}{2\pi}|1-\alpha k|^2, \tag{6.1}$$

where $k = (M^2 - M_1^2)/2M$, $\alpha = 0.5$ GeV^{-1}, and $g = 3.2$ GeV^{-1}. The lower curve is for $M = 5$ GeV, where $\langle n-1\rangle_{5\ \mathrm{GeV}} = 8.4$; the upper curve is for $M = 9$ GeV, and $\langle n-1\rangle_{9\ \mathrm{GeV}} = 15.1$. The low-$k_T$ distribution is essentially identical to that shown in Fig. 2. This is expected, since $|F(M^2, M_1^2)|^2$ in Eq. (6.1) is approximately constant for small k. For $M = 5$

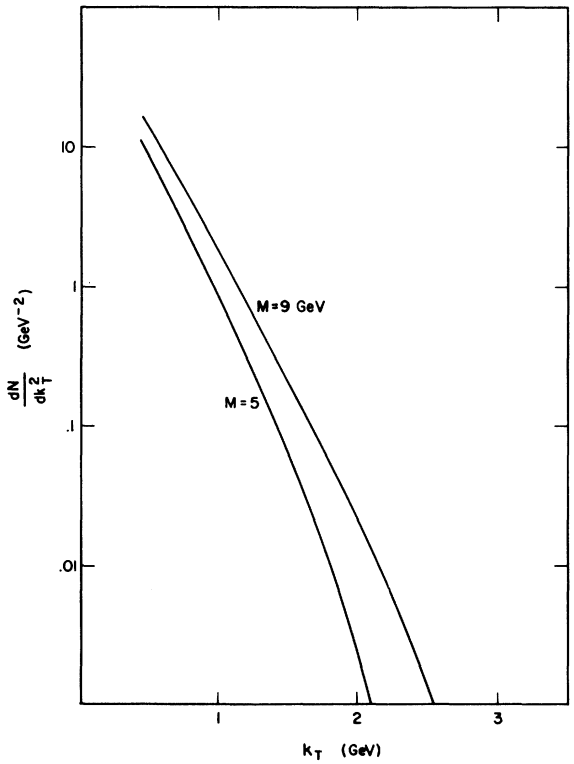

FIG. 2. Inclusive distributions for constant matrix element, $|F|^2 = g^2/2\pi$. The lower curve is dN/dk_T^2 for $M = 5$ GeV, the upper curve is dN/dk_T^2 for $M = 9$ GeV, where $g = 3.3$ GeV^{-1}.

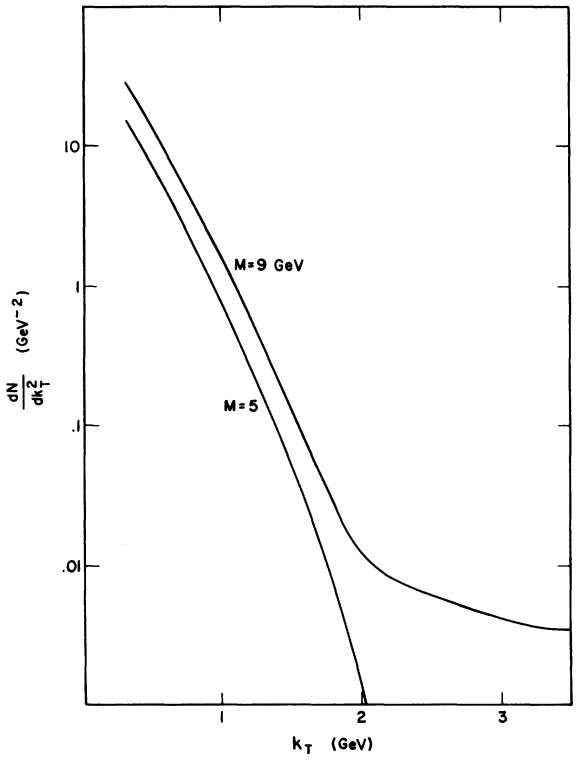

FIG. 3. Inclusive distribution dN/dk_T^2 for $|F|^2 = (g^2/2\pi)(1-\alpha k)^2$ with $g = 3.2$ GeV^{-1} and $\alpha = 0.5$ GeV^{-1}. The flattening of the $M = 9$ distribution is due to the dip in $|F|^2$ at $k = 2$ GeV, and is discussed in the text.

the zero in $|F|^2$ is close enough to the edge of phase space that it has little effect on the distribution. However, for $M=9$ GeV, the dip in $|F|^2$ has a pronounced effect on the momentum distributions of the first few particles emitted in the sequential decay. This flattening with M introduces the possibility of large-k_T fluxes and violations of scaling much larger than already imposed by the edge of phase space.

The flattening effect is easily understood in terms of $P(M_1|M)$, Eq. (5.4). For M large and k small ($k \ll M/2$), M_1 is large, $M_1 \approx M-k$, and we can approximate both of the functions $\Gamma(M_1^2)$ and $\Gamma(M^2)$ in $P(M_1|M)$ by their asymptotic forms, Eq. (4.10). With this approximation, $P(M_1|M)$ the probability for the emission of a secondary with momentum k is given to leading order in k/M by

$$P(M_1|M) \approx g^2 k(1-\alpha k)^2 e^{-\mu g k/2}, \quad k \ll M/2, \quad (6.2)$$

where $\mu = 1.213$ is the root of Eq. (4.11) with the largest positive real part. If M is large enough, the zero in $P(M_1|M)$ at $k = 1/\alpha = 2$ GeV is in the physical region $0 \leq k \leq M/2$ and $P(M_1|M)$ has two maxima, one at small k, and a second much smaller one at $k \approx 3$ GeV. The distribution Eq. (6.2) is, near its first maximum, quite similar to that for the constant matrix element with $g = 3.2$ GeV^{-1}. In the region near its second maximum and beyond, however, the distribution Eq. (6.2) is much larger than the corresponding distribution for a constant matrix element [$\alpha = 0$, $\mu \approx 2$ in Eq. (6.2)]. The result is (for M large) a greatly enhanced probability for the emission of secondaries with $k > 2$ GeV. This is reflected in the curves in Fig. 3. The dip in $P(M_1|M)$ is washed out by recoil effects in the sequential decay, and by the integration over k_L which converts $2E dN/dk^3$ to dk_T^2. However, the marked flattening of the distribution still begins near $k = 2$ GeV.

The extreme flattening effect at large k_T seems to occur only in models in which $|F|^2$ shows structure. There is no flattening, for example, for the matrix element

$$|F(M^2, M_1^2)|^2 = \frac{g^2}{2\pi}(1+\alpha k)^2, \quad \alpha > 0 \quad (6.3)$$

even though the large-k behavior of $|F|^2$ is similar to that of the matrix element in Eq. (6.1). The distribution $P(M_1|M)$ is almost identical in this case to that for a constant matrix element for $k < 3$ GeV, and actually falls below the constant case for larger values of k.

We consider as a second example the matrix element

$$|F(M^2, M_1^2)|^2 = \frac{g^2}{2\pi}\frac{1}{gk}. \quad (6.4)$$

In this case, $P(M_1|M)$ is given for large M and $k \ll M/2$ by

$$P(M_1|M) \approx g e^{-gk}, \quad k \ll M/2. \quad (6.5)$$

The inclusive distributions corresponding to this matrix element, for $g = 1.56$ GeV^{-1}, are shown in Fig. 4 for $M = 5$ GeV ($\langle n-1\rangle_{5\text{ GeV}} = 8.3$) and $M = 9$ GeV ($\langle n-1\rangle_{9\text{ GeV}} = 14.1$). The distributions are somewhat flatter for large k than those in Fig. 2, corresponding to the less steep fall of the exponential in Eq. (6.5) than that in Eq. (6.2) taken for $\alpha = 0$, $\mu = 2$, $g = 3.2$ (the case of a constant matrix element). However, the flattening is restricted to values of k_T well away from the edge of phase space at $k = M/2$, and is rather slight.

It is possible as in the previous example to obtain quite pronounced flattening of the inclusive distribution at large k_T by introducing a dip in the matrix element. For example, the matrix element

$$|F(M^2, M_1^2)|^2 = \frac{g^2}{2\pi}\frac{1}{gk}(1-\alpha k)^2 \quad (6.6)$$

with $\alpha = 0.425$ GeV^{-1}, $g = 1.7$ GeV^{-1}, gives the curves in Fig. 5. The lower curve ($M = 5$ GeV) has $\langle n-1\rangle_{5\text{ GeV}} = 9.1$; the upper curve ($M = 9$ GeV) has $\langle n-1\rangle_{9\text{ GeV}} = 14.9$. The dip in $|F|^2$ at $k = 2.35$ GeV

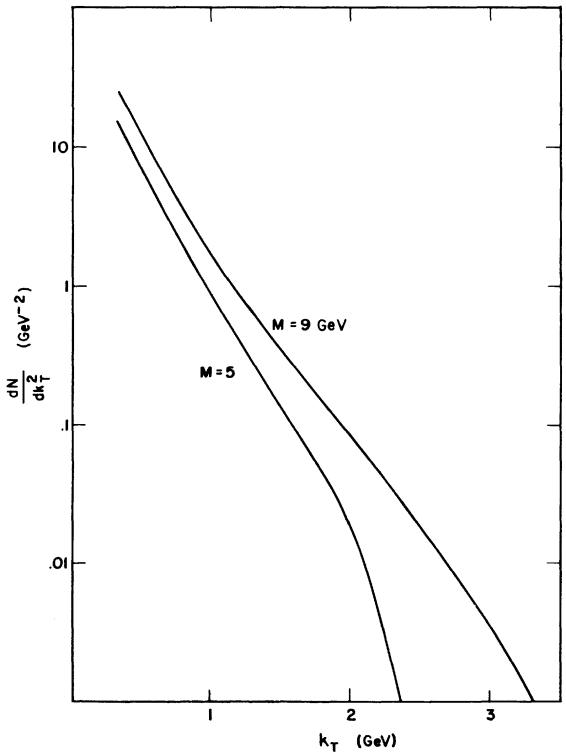

FIG. 4. Inclusive distribution, dN/dk_T^2, for $|F|^2 = g/(2\pi k)$, with $g = 1.56$ GeV^{-1}. The downward curvature at large k_T is similar to Fig. 2.

is close to the edge of phase space for $M=5$ GeV, and the 5-GeV curve is consequently quite similar to that in Fig. 4. For $M=9$ GeV, the inclusive distribution is quite flat for k beyond the dip, $k \gtrsim 2.3$ GeV.

We now return to a more complete discussion of the effect of the shape of $|F|^2$ on the shape of the momentum spectrum. In most of our models, $|F|^2$ increases for large $k=(M^2-M_1^2)/2M$. Of course, this does not mean that the probability for a secondary with large k also increases with k, since phase-space effects will decrease it. The correct indicator of the momentum spectrum is $P(M_1|M)$, given in Eq. (5.4). Even so, it may be a little surprising that two matrix elements with the same large-k limit, but different intermediate-k dependence, produce very different large-k_T spectra. We examine this in limits where $P(M_1|M)$ has a simple form.

Consider the limit of large M and M_1, with $k=(M^2-M_1^2)/2M \ll M_1$. For simplicity we consider $|F|^2$ of the form in Eq. (4.13),

$$|F|^2=\frac{g^2}{2\pi}\sum_n p_n g^n k^n. \tag{6.7}$$

Equation (5.4) for $P(M_1|M)$ contains $\Gamma(M_1^2)$ and $\Gamma(M^2)$, which we approximate by Eq. (4.10). Keeping terms to leading order in k/M ($M_1 \simeq M-k$), we find $P(M_1|M)$ to have the simple behavior

$$P(M_1|M)=\sum_n p_n g^{n+2} k^{n+1} \exp\left(-\frac{\mu g k}{2}\right), \tag{6.8}$$

where μ is the root with the largest positive real part discussed in Eq. (4.11). Normalization factors have not been dropped in Eq. (6.8). Thus we see that the large (but not too large) k behavior is controlled by both $\tilde{\mu}=\mu g/2$ and $|F|^2$.

The issue now is to compare $P(M_1|M)$ for different models at fixed M, k, and average multiplicity for different $|F|^2$. We also keep the k dependence of $|F|^2$ (location of zeros, etc.) similar in this comparison. The average multiplicity in the large-M limit is given by Eq. (4.12):

$$N(M)=\rho M, \qquad \rho=\left(\frac{d\mu}{d\lambda}g/2\right)_{\lambda=1}. \tag{6.9}$$

Thus g is varied from case to case according to

$$g=[2\rho/(d\mu/d\lambda)]_{\lambda=1}. \tag{6.10}$$

In order to keep the structure in Eq. (6.7) constant as we vary g, we define coefficients

$$a_n=p_n g^n, \tag{6.11}$$

which will be kept fixed as g is varied.

The problem now is to find an equation for $\tilde{\mu}=\mu g/2$ in Eq. (6.8) in which ρ and a_n are fixed. Equation (4.8) allows us to make the identification

$$A_{n,0}=2^n(n-1)!\,a_{n-2}/g^{n-2}, \tag{6.12}$$

so that the root equation, Eq. (4.11), becomes

$$\tilde{\mu}^I=\lambda g^2\sum_{n=1}^{I}(n-1)!\,a_{n-2}\,\tilde{\mu}^{I-n}. \tag{6.13}$$

This equation depends on g^2. An equation for g^2 is obtained by evaluating $d\mu/d\lambda$ from Eq. (4.11) and substituting it into Eq. (6.10),

$$\frac{1}{g^2}=\rho\lambda\sum_{n=1}^{I} n!\,a_{n-2}\,\tilde{\mu}^{-n-1}. \tag{6.14}$$

Finally, we eliminate g^2 from Eqs. (6.13) and (6.14) and find an equation for $\tilde{\mu}$:

$$\sum_n n!\,(\rho a_{n-2}-a_{n-1})\,\tilde{\mu}^{I-n}=0. \tag{6.15}$$

We may compute the exponential decrease in $P(M_1|M)$ by solving Eq. (6.15). Consider as an example Eq. (6.1), where $a_0=1$, $a_1=-2\alpha$, and $a_2=\alpha^2$. ($\alpha>0$ is the case with destructive interfer-

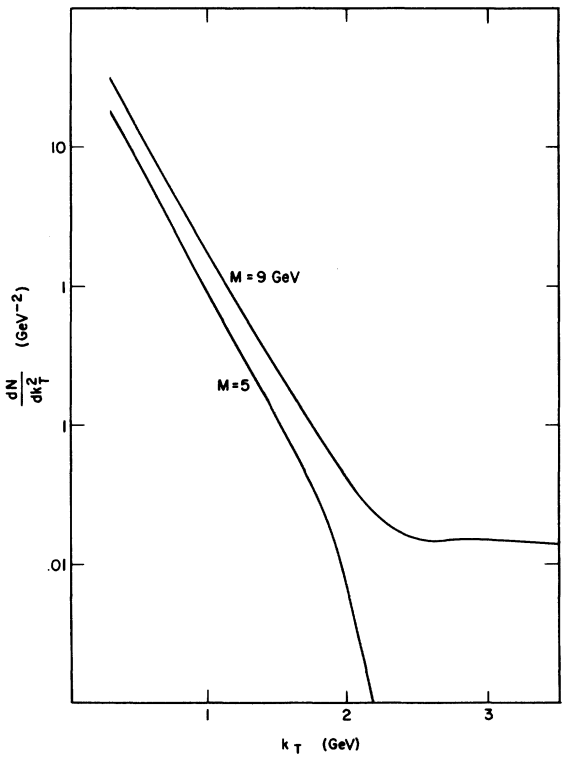

FIG. 5. Inclusive distribution, dN/dk_T^2, for $|F|^2=(g/2\pi k)(1-\alpha k)^2$ with $g=1.7$ GeV^{-1} and $\alpha=0.425$ GeV^{-1}. This again shows the flattening due to the effect of the dip which is located at $k=2.35$ GeV.

ence.) Equation (6.15) becomes

$$\tilde{\mu}^3 - 2(\rho+2\alpha)\tilde{\mu}^2 + 6\alpha(2\rho+\alpha)\tilde{\mu} - 24\rho\alpha^2 = 0. \quad (6.16)$$

In the calculation for Fig. 3, $\alpha = 0.5$ GeV^{-1} and $g = 3.2$ GeV^{-1}. This gives, from Eq. (6.13), $\tilde{\mu} = 1.94$ GeV^{-1} and from Eq. (6.14), $\rho = 1.424$. If we now change to $\alpha = -0.5$ GeV^{-1}, which is the case of constructive interference, we obtain from Eq. (6.16) $\tilde{\mu} \approx 3.53$ GeV^{-1}. [The value of g necessary to maintain $\rho = 1.424$ with this matrix element is, from Eq. (6.14), $g \approx 2.72$.] There is, therefore, a faster rate of falloff in the constructive interference case. The ratio of $P(M_1|M)$ for the two cases is proportional [up to the polynomial in Eq. (6.8)] to $\exp(-1.59\,k) \approx 1/33$ for $k = 2.2$ GeV. This accounts for the flattening of the $M = 9$ curve in Fig. 3.

In e^+e^- annihilation into hadrons, the mass of the presumed cluster is simply the e^+e^- center-of-mass energy. One can simply assume a phenomenological coupling for the photon to a spin-1 cluster and then study the correlation parameters (such as sphericity) which characterize the hadronic final states. It is, in fact, possible to give an accurate account of the sphericities and multiplicities with[5]

$$|F|^2 = \frac{g^2}{2\pi} k(1-\alpha k)^2(1-\beta k)^2, \quad (6.17)$$

where $1/\alpha = 0.82$ GeV, $1/\beta = 1.75$ GeV, and $g = 5.8$ GeV^{-1}.

The study of hadronic collisions is more complicated, since the clusters are produced with a spectrum of masses and longitudinal momenta. The detailed predictions of a model with a given decay matrix element will be sensitive to assumptions regarding the production mechanism. However, some general features are obvious. Because of the violations of scaling seen in Figs. 3 and 5, a large-k_T secondary is much more likely to have come from a high-mass cluster, even if the spectrum of high-mass clusters is somewhat suppressed. As a result, the multiplicity associated with these events should be higher than average. The violations of scaling are caused by the increasing effectiveness of the dips in $|F|^2$. More quantitative and detailed calculations are in progress.

ACKNOWLEDGMENT

We are grateful for the hospitality of the Aspen Center for Physics, where part of this work was done. We also thank many colleagues both at Los Alamos and at Aspen for helpful conversations and remarks.

APPENDIX

The results on the behavior of $\gamma(y)$ for large y which we used in Sec. IV were derived by considering the asymptotic solution of the recurrence relation given in Eq. (4.6) for $n \to \infty$ and the corresponding asymptotic behavior of the series in Eq. (4.2). We will summarize our results on the recurrence relation [Eq. (4.6)] in subsection 1, and we will use these results to determine the asymptotic behavior of the complete series [Eq. (4.2)] in subsection 2. In order to include the possibility of other than linear asymptotic growth of the multiplicity [see the remarks following Eq. (4.3)], we will actually consider series and recurrence relations somewhat more general than Eqs. (4.2) and (4.6). In subsection 3, we will discuss briefly some numerical problems associated with the series, and indicate how they can be avoided.

1. Asymptotic solutions of the recurrence relations

Let the function $f(x)$ be defined by the series

$$f(x) = \sum_{n=0}^{\infty} \frac{a_n x^n}{[\Gamma(n+1)]^b}, \quad b > 0. \quad (A1)$$

The expression for $\gamma(y)$ given in Eq. (4.2) corresponds to the choice $b = 1$. The coefficients a_n [or the g_n in Eq. (4.2)] are to be determined by a recurrence relation

$$a_n = \sum_{i=1}^{j} A_i(n) a_{n-i}, \quad n \geq j \quad (A2)$$

starting with given values for $a_0, \ldots, a_{j-1}$. Equation (4.6) gives the explicit form of the functions $A_i(n)$ considered in Sec. IV. These were rational functions of n which approached constants for $n \to \infty$.[9] We will assume here only that the $A_i(n)$ are such that they can be expanded in power series in n^{-1} for $n \to \infty$,

$$A_i(n) \sim \sum_{m=0} A_{i,m} n^{-m}, \quad n \to \infty \quad (A3)$$

with some of the $A_{i,0}$ nonzero.[10]

It is clear that the behavior of $f(x)$ for large x is determined primarily by the behavior of the coefficients a_n for large n. We can easily obtain asymptotic expansions of the a_n appropriate to this regime. For $n \to \infty$, the recurrence relation Eq. (A2) approaches the limiting form

$$a_n \sim \sum_{i=1}^{j} A_{i,0} a_{n-i}. \quad (A4)$$

We will suppose initially that this recurrence relation is exact, and will solve it exactly for a set of

coefficients $\bar{a}_n$ such that

$$\bar{a}_n = \sum_{i=1}^{j} A_{i,0}\,\bar{a}_{n-i}. \tag{A4'}$$

These coefficients will provide the starting point for our subsequent construction of an asymptotic solution to Eq. (A2).

The recurrence relation Eq. (A4') is equivalent to a jth-order difference equation, and has j independent solutions. These can be constructed by determining the j roots $\mu_{(l)}$ of the polynomial[11]

$$\mu^j = \sum_{i=1}^{j} A_{i,0}\,\mu^{j-i}. \tag{A5}$$

[This relation is equivalent to Eq. (4.12).] If the j roots $\mu_{(l)}$ are all distinct, the quantities $\bar{a}_n^{(l)} = c_l \mu_{(l)}{}^n$, with $l = 1, \ldots, j$ and c_l a constant, give j independent solutions to Eq. (A4'). The situation is only slightly more complicated if a root $\mu_{(p)}$ appears with multiplicity $m_p > 1$. The m_p independent solutions corresponding to $\mu_{(p)}$ are given by $\bar{a}_n^{(k,l)} = c_{kl} n^k \mu_{(p)}{}^n$, with $k = 0, \ldots, m_p - 1$.

Any solution a_n of the exact recurrence relation Eq. (A2) can always be expressed as a linear combination of j independent solutions $a_n^{(l)}$, $l = 1, \ldots j$,

$$a_n = \sum_{l=1}^{j} C_l\, a_n^{(l)}. \tag{A6}$$

We will fix the basic solutions $a_n^{(l)}$ by requiring that $a_n^{(l)}$ have the asymptotic behavior of the $\bar{a}_n^{(l)}$ constructed above, that is, $a_n^{(l)} \propto \mu_{(l)}{}^n$ for $n \to \infty$. This is always possible because Eq. (A4') is just the asymptotic form of the exact recurrence relation Eq. (A2). It is easy to see that the general solution to Eq. (A2) may also involve a power of n for $n \to \infty$, so that $a_n^{(l)} \propto n^{\alpha_l} \mu_{(l)}{}^n$. We will in fact show that Eq. (A2) can be solved to any finite order in n^{-1} by a coefficient with the asymptotic form

$$a_n^{(l)} \sim n^{\alpha_l} \mu_{(l)}{}^n \sum_{p=0} B_p^{(l)} n^{-p}, \quad n \to \infty. \tag{A7}$$

We will fix the normalization by choosing $B_0^{(l)} = 1$.

To establish this result, we substitute Eq. (A7) and the expansion of $A_i(n)$ given in Eq. (A3) in Eq. (A2), and collect powers of n^{-1}. We find that the recurrence relation Eq. (A2) is satisfied provided

$$\mu_{(l)}{}^j B_k^{(l)} = \sum_{i=1}^{j} \sum_{\substack{m,p,q=0 \\ m+p+q=k}} \binom{\alpha_l - p}{q} (-i)^q \mu_{(l)}{}^{j-1} \times A_{i,m} B_p^{(l)}, \tag{A8}$$

where $(\cdots)$ is a binomial coefficient. For $k = 0$, we have $m = p = q = 0$, and Eq. (A8) reduces simply to

$$\mu_{(l)}{}^j = \sum_{i=1}^{j} A_{i,0}\,\mu_{(l)}{}^{j-i}, \tag{A9}$$

that is, to the requirement that $\mu_{(l)}$ be a root of the polynomial Eq. (A5), as expected. This requirement is in fact sufficient to eliminate all the terms in Eq. (A8) with $m = q = 0$ for arbitrary $p = k$, and we need consider only the remainder of the expression with $m + q \geq 1$. For $k = 1$, this determines α_l,

$$\alpha_l = \left(\sum_{i=1}^{j} A_{i,1} \mu_{(l)}{}^{j-i}\right)\left(\sum_{i=1}^{j} i A_{i,0} \mu_{(l)}{}^{j-i}\right)^{-1}. \tag{A10}$$

The expressions for $k \geq 2$ determine the B's through the recurrence relation

$$B_k^{(l)} = -D_{k,k}{}^{-1} \sum_{p=0}^{k-1} D_{k,p} B_p^{(l)}, \quad B_0^{(l)} = 1 \tag{A11}$$

where

$$D_{k,p} = \sum_{q=0} (-1)^q \binom{\alpha_l - p}{q} \sum_{i=1}^{j} i^q A_{i,k-p-q+1}\, \mu_{(l)}{}^{j-i}. \tag{A12}$$

This recurrence relation can be used to find $B_k^{(l)}$ for arbitrary k in terms of $\mu_{(l)}$ and the $A_{i,m}$. We note finally that the expansion of $a_n^{(l)}$ given in Eq. (A7) is generally only asymptotic, and should be truncated after a few terms.

2. Asymptotic estimates of the series

The function $f(x)$ defined in Eq. (A1) can be written as

$$f(x) = \sum_{l=1}^{j} C_l\, f_l(x), \tag{A13}$$

where

$$f_l(x) = \sum_{n=0}^{\infty} \frac{a_n^{(l)} x^n}{[\Gamma(n+1)]^b}. \tag{A14}$$

As noted previously, the asymptotic form of $f_l(x)$ for $x \to \infty$ is determined by the asymptotic form of the coefficients $a_n^{(l)}$. For simplicity, we will retain only the leading term in the asymptotic expansion of these coefficients given in Eq. (A7), and will approximate $f_l(x)$ by

$$f_l(x) \sim \sum_n \frac{n^{\alpha_l} z_l^n}{[\Gamma(n+1)]^b}, \quad b > 0, \quad |z_l| = |\mu_{(l)} x| \to \infty. \tag{A15}$$

The correction terms involve extra inverse powers of n.

The simplest case to consider is that in which $z_l = \mu_{(l)} x$ is real and positive. We can use Stirling's approximation for the Γ function to write the series as

$$f_l(x) \sim (2\pi)^{-b/2} \sum_n e^{\phi_l(n)}, \tag{A16}$$

$$\phi_l(n) \approx -b(n+\tfrac{1}{2}) \ln n + bn + n \ln z_l + \alpha_l \ln n + O(n^{-1}), \tag{A17}$$

and can approximate the sum by an integral,

$$f_l(x) \sim (2\pi)^{-b/2} \int e^{\phi_l(n)} dn. \tag{A18}$$

The integrand has a saddle point [maximum of $\phi(n)$] at the point $n = n_l$,

$$n_l \approx z_l^{1/b} \left[1 + z_l^{-1/b}\left(\frac{\alpha_l}{b} - \tfrac{1}{2}\right) + \cdots\right], \tag{A19}$$

and can be estimated by using the method of steepest descent.[12] The result is quite simple,[13]

$$f_l(x) \sim (2\pi)^{-(b-1)/2} b^{-1/2} z_l^{(2\alpha_l - b + 1)/2b} \times e^b z_l^{1/b}[1 + O(z_l^{-1/b})], \quad z_l \text{ real}, \quad z_l \gg 1. \tag{A20}$$

The correction terms are associated both with the approximation of the integral, and with the neglect of the expansion in inverse powers of n in Eq. (A7). For the case of interest in Sec. IV, $b = 1$, and

$$f_l(x) \sim z_l^{\alpha_l} e^{z_l}, \quad z_l = \mu_{(l)} x \gg 1. \tag{A21}$$

If $\mu_{(l)}$ is complex or negative, the terms in the series for $f_l(x)$ oscillate in sign, and we cannot simply replace the sum by an integral over positive n as above. However, we can convert the series into an exact contour integral by using the Sommerfeld-Watson transformation,[14] and can estimate the integral for $|z_l|$ large by using the method of steepest descent and the asymptotic form of the integrand. We find that the result in Eq. (A20) continues to hold for complex z_l with $|\arg z_l| < b\pi/2$. With this restriction, the argument of z_l is such that $\mathrm{Re}\, z_l^{1/b} > 0$, and the absolute magnitude of the exponential in Eq. (A20) increases as $|z_l|$ increases with $\arg z_l$ fixed.

It is unfortunately not possible to obtain reliable results for $f_l(x)$ for $\mathrm{Re}\, z_l^{1/b} < 0$ using the present methods. While the expressions above suggest that $f_l(x)$ will behave as a power of $z^{1/b}$ multiplied by a decreasing exponential in this region, there may be extra nonexponential contributions associated with the first few nonasymptotic terms in the series Eq. (A14).[15] We cannot estimate these contributions without more detailed knowledge about the $a_n^{(l)}$ than we have used.

For the case of interest in Sec. IV, $b = 1$, and $f_l(x)$ has the asymptotic form given in Eq. (A21), provided $|\arg z_l| < \pi/2$. The asymptotic form of the complete series $f(x) = \sum_{l=1}^{j} C_l f_l(x)$ is determined in this case by the root of Eq. (A5) with largest positive real part. For the class of models we have considered, it is rather easy to show that the positivity of $|F|^2$ ensures the existence of at least one positive real root, hence an exponential growth of $f(x)$ [or $\gamma(y)$] as $x \to \infty$ ($y \to \infty$).

3. Numerical treatment of the series

The numerical characteristics of the series Eq. (A1) depend primarily on the roots $\mu_{(l)}$ of Eq. (A5). We have seen that the coefficients a_n can be expressed as

$$a_n = \sum_{l=1}^{j} C_l a_n^{(l)}, \tag{A22}$$

where the $a_n^{(l)}$ behave asymptotically as

$$a_n^{(l)} \sim n^{\alpha_l} \mu_{(l)}{}^n, \quad n \to \infty. \tag{A23}$$

The largest contributions to a_n are associated with the roots with the largest absolute magnitudes. However, Eq. (A20) shows that the dominant contribution to $f(x)$ for real x is associated with the root with the algebraically largest real part (we will restrict our attention to the case $b = 1$ considered in Sec. IV). These roots differ for a large class of interesting models of the type considered in Sec. IV, especially those with strong destructive interference in the matrix element.

As a simple example, consider the model with $|F|^2 = (g^2/2\pi)(1 - gk)^2$. The function $\gamma(y)$ defined by Eq. (4.2) with $\lambda = 1$ is given in this case by a series of the form Eq. (A1) with $\beta = 1$, and series coefficients g_n determined by Eq. (4.14b) and Eq. (4.15). The asymptotic recurrence relation for g_n is

$$g_n = 4g_{n-2} - 32g_{n-3} + 96g_{n-4}. \tag{A24}$$

The corresponding asymptotic polynomial and its roots are

$$\mu^4 = 4\mu^2 - 32\mu + 96,$$
$$\mu_1 = 2.525\,70, \quad \mu_2 = 0.814\,54 + 2.912\,82i, \tag{A25}$$
$$\mu_3 = 0.814\,54 - 2.912\,82i, \quad \mu_4 = -4.154\,86.$$

The asymptotic behavior of the coefficients g_n is determined by μ_4, and to a lesser extent, by μ_2 and μ_3. However, the series which involves μ_2, μ_3, and μ_4 sums to functions $\gamma_1(y)$, $\gamma_3(y)$, and $\gamma_4(y)$, which are exponentially small compared to $\gamma_1(y)$ for large y by Eq. (A21). In the present example, $\gamma_1(y) \sim 10^7$ for $y \approx 10$, $|\gamma_2(y)| = |\gamma_3(y)| \sim 10^3$, and $\gamma_4(y) \sim 10^1$. However, note that the largest terms in the series for $\gamma_4(y)$ have a magnitude $\sim 10^{14}$, 10^7 times larger than the entire function $\gamma(y)$.

The foregoing situation is typical for the large-multiplicity region in models with strong destructive interference. The function obtained by summing the series $\sum_n |g_n| y^n/n!$ instead of the series

$\sum_n g_n y^n/n!$ for $\gamma(y)$ is usually $\sim 10^6$–10^8 times larger than $\gamma(y)$ for multiplicities of 8–15, indicating a loss of ~6–8 significant figures in $\gamma(y)$ because of cancellations. We have therefore found it necessary to use double-precision arithmetic to obtain meaningful results in our calculations.

It is possible to reorganize the calculation of a general $f(x)$ of the form Eq. (A1) in a manner which circumvents the problem above by splitting f into the functions f_l with the definite asymptotic behaviors specified by Eq. (A20). The individual series can then be calculated separately, and only the dominant series need be considered for x large. Thus, in the example above, we could calculate γ_4 without difficulty for y small, and could drop it altogether when it becomes negligible relative to γ_1.

The splitting of the series is relatively simple. The problem is one of finding j linearly independent sets of characteristic starting values $a_0^{(l)}, \ldots, a_{j-1}^{(l)}, l = 1, \ldots, j$, for the recurrence relation Eq. (A2) such that the lth set gives as asymptotic coefficient with the unique n dependence $a_n \sim a_n^{(l)}$, Eq. (A7). Once these are found, the known starting values $a_0, \ldots, a_{j-1}$ can be expressed in terms of the characteristic values $a_j^{(l)}$ and a set of j constants C_l determined by the j equations

$$a_i = \sum_{l=1}^{j} C_l a_i^{(l)}, \quad i = 0, \ldots, j-1. \tag{A26}$$

The function $f(x)$ is then given by

$$f(x) = \sum_{l=1}^{j} C_l f_l(x), \tag{A27}$$

where $f_l(x)$ is given by the series Eq. (A1) with the coefficients calculated using the exact recurrence relation Eq. (A2) and the characteristic starting set $a_i^{(l)}$, $i = 0, \ldots, j-1$.

The characteristic starting values $a_i^{(l)}$ can be determined trivially for small roots, $|\mu_{(l)}| \sim 1$, by starting with j successive values of the asymptotic coefficient $a_n^{(l)}$ say $a_N^{(l)}$, $a_{N+1}^{(l)}, \ldots, a_{N+j-1}^{(l)}$, and using the exact recurrence relation Eq. (A2) in the backward sense. The overall normalization of the coefficients $a_0^{(l)}, \ldots, a_{j-1}^{(l)}$ determined in this way is arbitrary. The starting value N should be large enough that the series $f_p(x)$ corresponding to the root with the largest positive real part will converge to the desired accuracy when only N terms are retained, and x has its maximum value. This value of N is easily estimated using the asymptotic expression Eq. (A20).

The foregoing method may fail for the large roots because of the cancellations which occur in the backward recurrence scheme for $|\mu_l| \gg 1$. In this case, we can determine the characteristic starting values as follows. We first choose $j-k$ sets of coefficients $a_{0,r}, \ldots, a_{j-1,r}$, $r = k, \ldots, j-1$, which are linearly independent of each other and of the k sets determined above. These are used to generate sets of asymptotic coefficients $a_{n,r}$ for $n = N, \ldots, N + j - 1$ by using the recurrence relation in the forward direction. The coefficients in each set can be expressed as linear combinations of the asymptotic coefficients $a_n^{(l)}$ given in Eq. (A7) for $l = k+1, \ldots, j$. (The $a_n^{(l)}$ for $l = 1, \ldots, k$ do not contribute by construction.) That is, we determine a set of coefficients $c_{r,l}$ for each value of r such that

$$a_{n,r} = \sum_{l=k+1}^{j} c_{r,l} a_n^{(l)}, \tag{A28}$$

$$n = N, \ldots, N+j-1, \quad l = k+1, \ldots, j.$$

Finally, we express the $a_n^{(l)}$ in terms of the $a_{n,r}$ by inverting the matrix of coefficients $c_{r,l}$,

$$a_n^{(l)} = \sum_{r=k}^{j-1} (c^{-1})_{lr} a_{n,r}. \tag{A29}$$

This relation implies that the characteristic starting values $a_i^{(l)}$ associated with the lth root are given in terms of our arbitrary starting sets $a_{0,r}, \ldots, a_{j-1,r}$ by

$$a_i^{(l)} = \sum_{r=k}^{j-1} (c^{-1})_{lr} a_{i,r}, \quad i = 0, \ldots, j-1. \tag{A30}$$

---

*Work supported by the U. S. Energy Research and Development Administration under Contracts Nos. W-7405-ENG-36 and COO-881, in part by the National Science Foundation under Grant No. MPS-72-05166-A01, and in part by the University of Wisconsin Research Committee with funds granted by the Wisconsin Alumni Research Foundation.

†Permanent address: Department of Physics, University of Wisconsin, Madison, Wisconsin 53706.

‡Permanent address.

[1]For reviews of multiparticle production, see L. Van Hove, Phys. Rep. 1C, 347 (1971); W. Frazer *et al.*, Rev. Mod. Phys. 44, 284 (1972); R. Slansky, Phys. Rep. 11C, 99 (1974); L. Foà, *ibid.* 22C, 1 (1975).

[2]G. Hanson *et al.*, Phys. Rev. Lett. 35, 1609 (1975).

[3]C. Quigg, P. Pirilä, and G. Thomas, Phys. Rev. Lett. 34, 290 (1975); T. Ludlam and R. Slansky, Phys. Rev. D 12, 59 (1975).

[4]D. Sivers, S. Brodsky, and R. Blankenbecler, Phys. Rep. 23C, 1 (1976).

[5]T. Goldman and R. Slansky, Los Alamos Report No. LA-UR-76-1472, 1976 (unpublished).

[6]E. Byckling and K. Kajantie, *Particle Kinematics* (Academic, New York, 1971).

[7]Equations of this type have also been studied by I. Montvay, Nucl. Phys. B53, 521 (1973).

[8]For a general discussion of Monte Carlo event generators, see Ref. 6. L. Van Hove, Nucl. Phys. B9, 331 (1969) is the basis of the CERN program FOWL, which is discussed in detail by F. James, CERN Computer Program Library (1970). Another event generator has been devised by M.-S. Chen and R. F. Peierls, J. Comput. Phys. 16, 195 (1974).

[9]We remind the reader that growth of the $A_j(n)$ with $n \to \infty$ would correspond in the applications in Sec. IV to an unphysical, faster-than-linear growth of the multiplicity with the cluster mass.

[10]If all of the $A_{i,0}$ vanish, we can extract a power of $(n!)^{-1}$ from the coefficients, and bring the recurrence relation to a form similar to Eq. (A2) with some of the modified functions $A'_i(n)$ finite for $n \to \infty$. The asymptotic form of modified coefficients a'_n can be determined using methods similar to those used below. The most important change is the replacement of $\mu_{(l)}{}^n$ in Eq. (A7) by $\mu_{(l)}{}^{n+n'}$, where n'/n can be expressed as a series of inverse fractional powers of n.

[11]We will assume for simplicity that $A_{j,0} \neq 0$. If $A_{j,0}$ vanishes, one of the roots of Eq. (A5), say μ_j, is zero, and the corresponding solution for a_n is trivial. In this case, the jth independent solution to the exact recurrence relation Eq. (A2) vanishes for $n \to \infty$, and can only be determined by considering the terms of order n^{-1}, which were dropped in going from Eq. (A2) to Eq. (A4). An analysis similar to that which follows Eq. (A6) shows that $a_n^{(j)}$ behaves in this case as

$$a_n^{(j)} = A_j(-A_{j,1}/A_{j-1,0})^n \frac{n^{\alpha_j}}{n!} \sum_{p=0} B_p n^{-p}, B_0 = 1$$

where α_j and the B's for $p \geq 1$ can be determined by requiring that Eq. (A2) be satisfied to a given order in n^{-1}. Note that $a_n^{(j)}$ vanishes more rapidly than exponentially for $n \to \infty$, hence the appearance of the zero root of Eq. (A5).

[12]P. M. Morse and H. Feshbach, *Methods of Theoretical Physics* (McGraw-Hill, New York, 1953), Vol. 1, p. 437 ff.

[13]This result reproduces known results in many special cases. For example, the series for $(2/x)^\nu I_\nu(x)$ may be approximated as

$$(2/x)^\nu I_\nu(x) = \sum_{n=0}^{\infty} \frac{(x/2)^{2n}}{\Gamma(n+1)\Gamma(n+\nu+1)}$$

$$\approx \sum_n \frac{n^{-\nu}(x/2)^{2n}}{[\Gamma(n+1)]^2} .$$

We conclude from this expression, Eq. (A15), and Eq. (A21) that the modified Bessel function $I_\nu(x)$ has the asymptotic form

$$I_\nu(x) \sim (2\pi x)^{-1/2} e^x ,$$

which is a standard result.

[14]G. N. Watson, Proc. R. Soc. London 95, 83 (1918); A. Sommerfeld, *The Partial Differential Equations of Physics* (Academic, New York, 1949), p. 282.

[15]For example, Eq. (A21) gives the correct asymptotic estimate e^x for the series $e^x - 1 = \sum_{n=1}^{\infty} x^n/n!$, $x > 0$, but fails completely for the series $e^{-x} - 1 = \sum_{n=1}^{\infty} (-x)^n/n!$. The dominant asymptotic term in the latter case is -1, not e^{-x}.